

# Precipitation of Iron Oxide in Hydrogel with Superparamagnetic and Stimuli-Responsive Properties <sup>†</sup>

Alice Mieting <sup>1,\*</sup>, Sitao Wang <sup>1</sup>, Mia Schliephake <sup>2</sup>, Daniela Franke <sup>1</sup> , Margarita Guenther <sup>1</sup> , Stefan Odenbach <sup>2</sup> and Gerald Gerlach <sup>1</sup> 

<sup>1</sup> Faculty of Electrical Engineering and Information Technology, Institute of Solid State Electronics, Dresden University of Technology, 01069 Dresden, Germany; sitao.wang@tu-dresden.de (S.W.); daniela.franke@tu-dresden.de (D.F.); margarita.guenther@tu-dresden.de (M.G.); gerald.gerlach@tu-dresden.de (G.G.)

<sup>2</sup> Faculty of Mechanical Engineering, Institute of Mechatronical Mechanical Engineering, Dresden University of Technology, 01069 Dresden, Germany; mia.schliephake@tu-dresden.de (M.S.); stefan.odenbach@tu-dresden.de (S.O.)

\* Correspondence: alice.mieting@tu-dresden.de

<sup>†</sup> Presented at the 1st International Electronic Conference on Chemical Sensors and Analytical Chemistry, 1–15 July 2021; Available online: <https://sciforum.net/conference/CSAC2021>.

**Abstract:** In this work, we present a template-based preparation of iron oxide-containing hydrogels (ferrogels) with ionic sensitive and superparamagnetic properties. The influence of the cross-linked template polyacrylamide and the concentration of the iron salts and sodium hydroxide on the precipitation of the iron oxide particles is investigated with respect to the stability of the ferrogels. Scanning electron microscope images show cubic particles, which can be semiquantitatively classified in three groups of particle size with respect to the dilution level. Magnetic hysteresis curves reveal a sigmoidal shape without remanence and coercivity for all samples. The higher cross-linked ferrogels, in comparison with the lower cross-linked ferrogels, possess a steady-state degree of swelling in ultrapure water and a stimuli-sensitive deswelling over a wide range of varying ionic strengths. Thus, they are suitable candidates for applications in sensing and microfluidics.

**Keywords:** stimuli-responsive hydrogel; superparamagnetic; iron oxide; coprecipitation; ferrogel



**Citation:** Mieting, A.; Wang, S.; Schliephake, M.; Franke, D.; Guenther, M.; Odenbach, S.; Gerlach, G. Precipitation of Iron Oxide in Hydrogel with Superparamagnetic and Stimuli-Responsive Properties. *Chem. Proc.* **2021**, *5*, 49. <https://doi.org/10.3390/chemproc2021005049>

Academic Editor: Nicole Jaffrezic-Renault

Published: 17 December 2021

**Publisher's Note:** MDPI stays neutral with regard to jurisdictional claims in published maps and institutional affiliations.



**Copyright:** © 2021 by the authors. Licensee MDPI, Basel, Switzerland. This article is an open access article distributed under the terms and conditions of the Creative Commons Attribution (CC BY) license (<https://creativecommons.org/licenses/by/4.0/>).

## 1. Introduction

Hydrogels are cross-linked, usually hydrophilic polymers, which are suitable candidates for applications in sensor [1] and actuator technology [2] due to their stimuli-sensitive swelling and viscoelastic properties. The incorporation of iron oxide particles into hydrogels results in novel composite materials with enhanced chemical and physical properties. Various approaches have demonstrated the sensitive and adsorptive properties of iron oxide particles with respect to heavy metal ions [3–5], pH [6], and biomolecules [7,8], as well as photocatalytic activity [9,10].

The aim of this work is the investigation of how the mechanical stability of the template structure and the concentration of the synthesis solutions influence the properties of in situ precipitated iron oxide particles. Understanding the structure–property relations of such novel composite materials relates to ongoing topics of scientific applications and research in engineering [11] and biomedicine [12] as well as in the treatment of contaminated water [13].

In this study, the wet chemical precipitation of iron oxides from iron salts with sodium hydroxide in the stoichiometric ratio of magnetite ( $\text{Fe}^{\text{II}}(\text{Fe}^{\text{III}})_2\text{O}_4$ ) is investigated in two various cross-linked hydrogels: a higher cross-linked hydrogel, which has already been used in piezoresistive sensors [14], named sensor hydrogel/ferrogel, and a lower cross-linked hydrogel, which is used in actuator setups [15], named actuator hydrogel/ferrogel

(Figure 1A). It is expected that in template-based precipitation the differently crosslinked hydrogels will affect the particle shape and size and in turn the swelling properties as well as the magnetic properties of the resulting ferrogels. On the other hand, different dilution levels of iron salts and sodium hydroxide will be used to investigate a suitable synthesis concentration with respect to the sensitivity and stability of the ferrogels (Figure 1B).

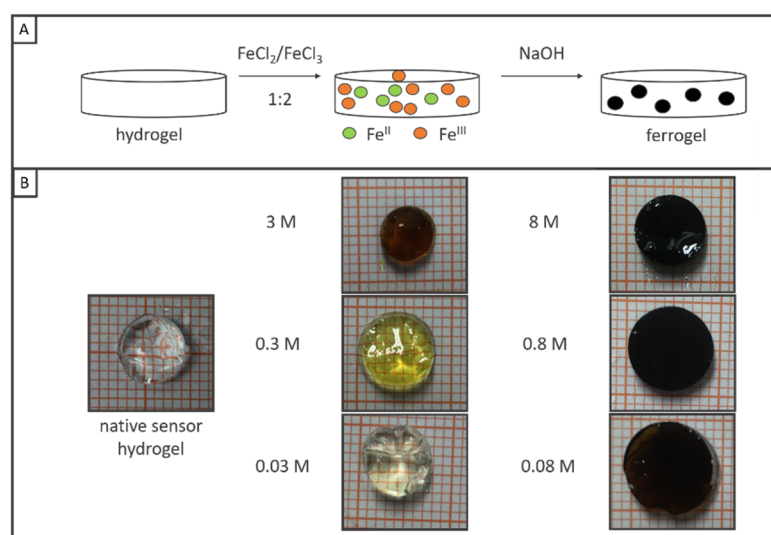


**Figure 1.** Scheme of the precipitation of iron oxide in hydrogel using iron chloride and sodium hydroxide solutions (A). Overview of the transformation of a sensor hydrogel to a ferrogel by soaking the samples in iron salt solution with orange-yellow coloring and forming black-brown-colored ferrogels in sodium hydroxide at different dilution levels (B).

## 2. Materials and Methods

### 2.1. Synthesis of Iron Oxide in Hydrogels

The monomer acrylamide (AAM), crosslinker *N,N'*-methylene-bis-acrylamide (BIS), ammonium peroxodisulfate (APS), ferric chloride hexahydrate ( $\text{FeCl}_3 \cdot 6\text{H}_2\text{O}$ ), ferrous chloride tetrahydrate ( $\text{FeCl}_2 \cdot 4\text{H}_2\text{O}$ ), and sodium chloride (NaCl) were purchased from Sigma-Aldrich, Saint Louis, MO, USA. *N,N,N',N'*-tetramethylethylenediamine (TEMED) was purchased from Carl Roth, Karlsruhe, Germany.

#### 2.1.1. Sensor Hydrogels

For the synthesis of sensor hydrogel, 1.6 M (8 mmol, 0.5686 g) AAm and 1.5 mol% (0.12 mmol, 0.0185 g) BIS were dissolved in 4.156 mL ultrapure water and placed in an ice bath to cool. Polymerization was initiated by adding 300  $\mu\text{L}$  of 0.072 M APS solution (0.022 mmol APS) and 2.1 mol% (0.168 mmol, 25.4  $\mu\text{L}$ ) TEMED. The cooled solution was placed in glass tubes with a diameter of about 6 mm, sealed, and left overnight at room temperature for polymerization. The polymerized polyacrylamide (PAAm) hydrogels were removed from the glass tubes and washed in ultrapure water for 5 days. Discs of about 2 mm thickness were cut from each of the cylindrical samples for in situ precipitation of the iron oxides in hydrogel.

#### 2.1.2. Actuator Hydrogels

The actuator hydrogel was synthesized and handled in the same procedure as the sensor hydrogel, but with the following composition: 2.8 M (14 mmol, 1.0 g) AAm and 0.03 mol% (4.2  $\mu\text{mol}$ , 0.7 mg) BIS were dissolved in 3.8 mL ultrapure water. Polymerization was initiated by adding 300  $\mu\text{L}$  of 0.15 M APS solution (0.045 mmol APS) and 0.48 mol% (0.1 mmol, 10.2  $\mu\text{L}$ ) TEMED.

### 2.1.3. Coprecipitation of Iron Oxide in Hydrogels

In order to prepare for precipitation, the sliced native hydrogel discs were rinsed with nitrogen in ultrapure water free of oxygen.

The first step was to disperse the iron chloride solution into the hydrogel. Thus, 12 mL of a 3 M mixture of iron (III) chloride hexahydrate (24 mmol, 6.4870 g) and iron (II) chloride tetrahydrate (12 mmol, 2.3860 g) was prepared in a 2:1 molar ratio. After that, a 1:10 dilution and a 1:100 dilution, each in 10 mL, were made from the 3 M iron salt solution. Each sensor and actuator hydrogel was placed in 5 mL of the appropriate iron chloride concentration for 24 h.

For the precipitation of iron oxide, 12 mL of an 8 M sodium hydroxide solution (96 mmol, 3.8397 g) was prepared, and a 1:10 dilution and a 1:100 dilution, each in 10 mL, were made from it. The iron salt-soaked hydrogels were transferred to 5 mL of the appropriate concentration of sodium hydroxide and left overnight. Finally, the ferrogels were washed until the pH of the water was neutral.

In general, the precipitation was performed under nitrogen atmosphere, and all solutions and the ultrapure water were used in a degassed condition. However, the following experiments and investigations were carried out to characterize the hydrogels under ambient conditions so that oxidation of magnetite ( $\text{Fe}_3\text{O}_4$ ) to maghemite ( $\gamma\text{-Fe}_2\text{O}_3$ ) is suggested.

## 2.2. Characterization Methods

### 2.2.1. Scanning Electron Microscopy (SEM)

A piece of each sample was air-dried and sputtered with a 5 nm thick gold layer for subsequent secondary electron imaging of the embedded iron oxide particles with a SEM (Zeiss Supra 40VP; Schottky emitter) at a fixed stage width and 7 keV.

### 2.2.2. Vibrating Sample Magnetometer (VSM)

The magnetization of the air-dried samples was measured on a Lake Shore VSM 7407 in the magnetic field range of  $\pm 17.5$  kOe at room temperature.

### 2.2.3. Swelling Experiments

In order to measure the impact of the changed environmental conditions on the hydrogels, the respective masses of the samples were weighed before and after addition of the stimulus. Without stimulus, the sample was in ultrapure water and had a mass  $m_0$ . The mass  $m_i$  of the sample with stimulus was determined after 24 h or after the corresponding long-term point. The degree of swelling was calculated as follows:

$$Q = \frac{m_i - m_0}{m_0} \times 100\%. \quad (1)$$

## 3. Results and Discussion

### 3.1. Morphological Properties

The scanning electron microscope images in Figure 2 of the sensor and actuator ferrogels of each dilution level show cubic particles between 50 and 300 nm and, in some cases, 1  $\mu\text{m}$  in size. Sensor and actuator ferrogels of undiluted concentrations (Figure 2a,b) and the actuator ferrogel of dilution level 1:10 (Figure 2e) additionally exhibit particles smaller than 20 nm distributed in the sample in a lawnlike manner and cannot be resolved with the currently used equipment. Due to the nonplanar arrangement of the particles, quantitative evaluation was not performed.

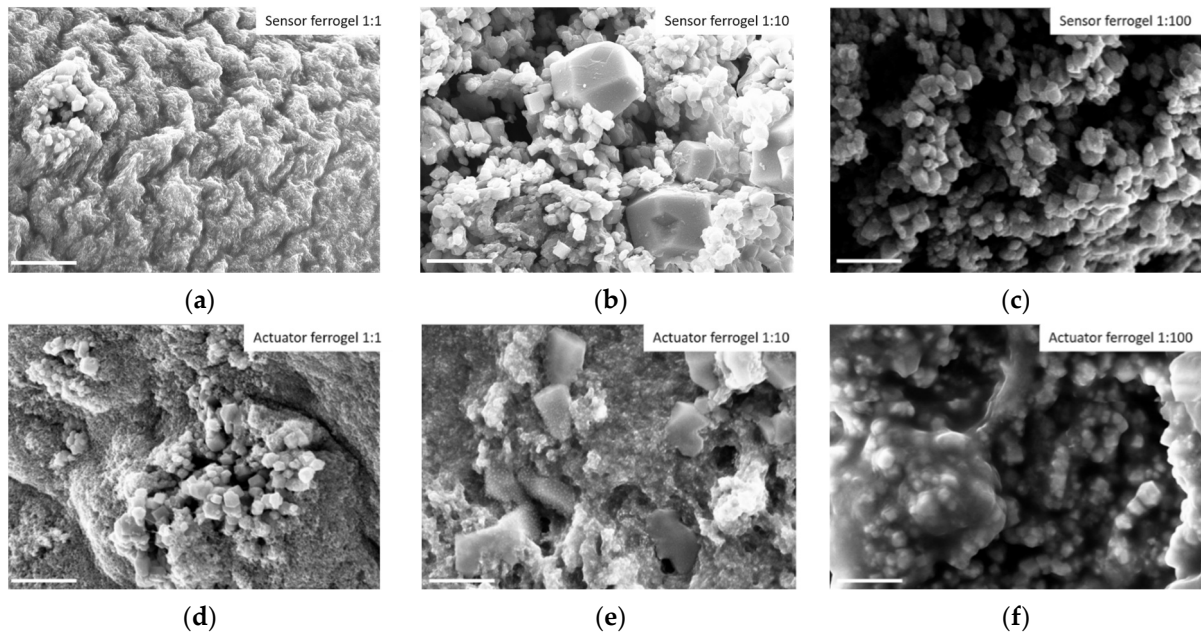


**Figure 2.** Representative SEM images of sensor ferrogels (a–c) and actuator ferrogels (d–f) of the different dilution levels. Scale bar: 1  $\mu\text{m}$ .

### 3.2. Magnetic Properties

Magnetization curves with an S-shaped profile without hysteresis gaining magnetic saturation characterize superparamagnetic behavior [16,17]. For all prepared ferrogels, the magnetization curves show a sigmoidal curve shape without coercivity and without remanence (Figure 3).

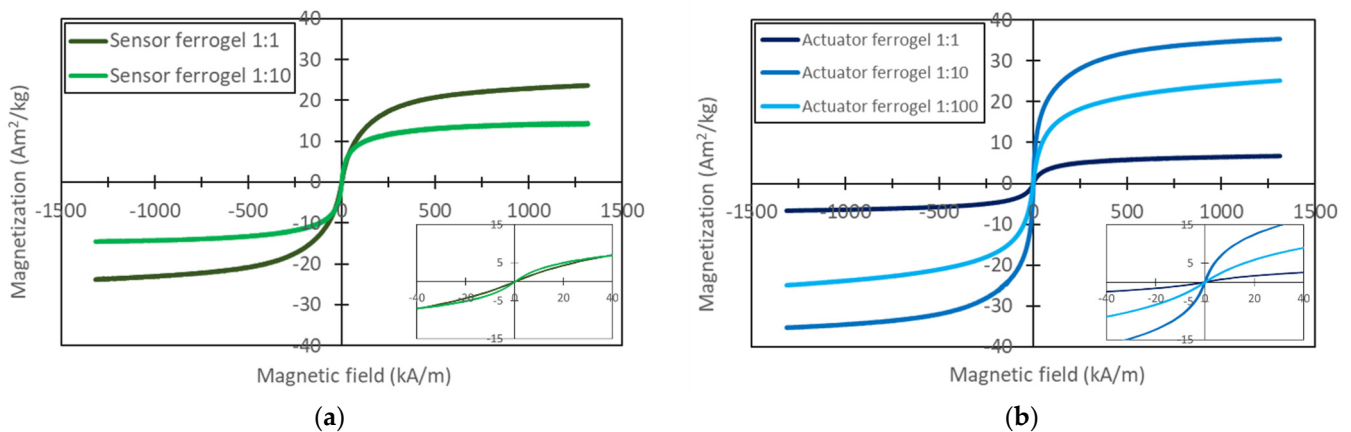


**Figure 3.** Magnetic hysteresis loop of the sensor ferrogels (a) and the actuator ferrogels (b) of the different dilution levels. Inset in the diagrams shows the curves at a low magnetic field.

The magnetization curve for the sensor ferrogel of dilution level 1:100 is not plotted in Figure 3a because the mass of this sample could not be determined due to sample instability in the dried state, making a quantitative comparison of the curves impossible. Except for the actuator ferrogel of dilution level 1:1, the saturation magnetization in both ferrogel types decreases with the dilution level, reflecting the lower content of magnetic particles in the ferrogel.

### 3.3. Reversibility of Ferrogel Swelling

Figure 4 depicts the swelling degrees of the ferrogels and native hydrogels alternating in ultrapure water and 1 M NaCl. Both ferrogels show a deswelling of around 80% in

solution with increased ionic strength. It can be concluded that in aqueous solution, the ferrogels are in the swollen state due to electrostatic repulsions of charged surface groups of the iron oxides. An increased ionic strength in the solution leads to electrostatic neutralization of the ionized groups of the iron oxide with the dissolved ions.

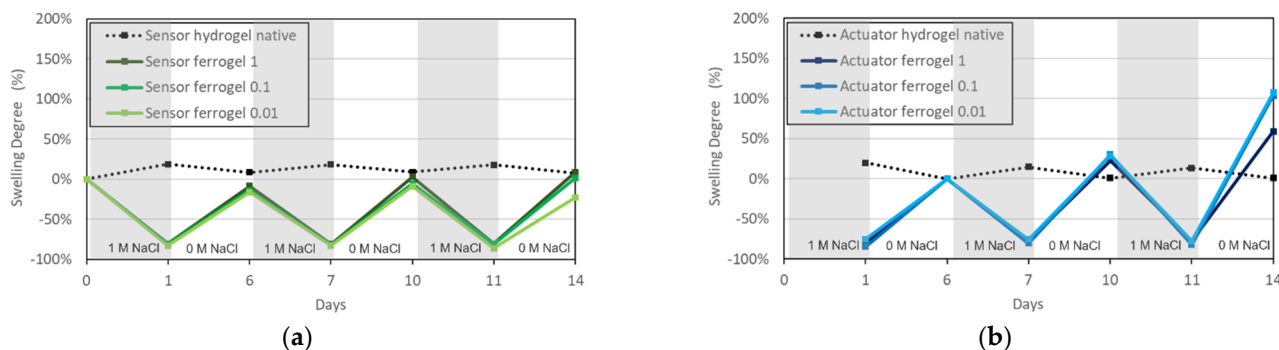


**Figure 4.** Swelling cycles showing the repeatability of the deswelling in 1 M NaCl solution and swelling in ultrapure water (0 M NaCl) of the sensor ferrogels (a) and actuator ferrogels (b).

Deswelling of the ferrogel occurs due to a reduction in electrostatic repulsions within the composite material comparable to the swelling behavior of pH or ion-sensitive hydrogels with fixed ionic groups in the polymer network [18]. In contrast, the native hydrogels show minor swelling under increased ionic strength due to osmotically induced swelling mechanisms.

The sensor ferrogels obtain their initial steady-state degree of swelling in water after three water/NaCl cycles (Figure 4a).

Due to the increased volume in water after synthesis, it was not possible to remove the actuator ferrogels from the sample containers so that detecting the mass could just start in the deswollen state. Furthermore, the actuator ferrogels show an increase in swelling degree during the second cycle in water and reach a swelling degree up to 50–100% in the third water cycle (Figure 4b).

### 3.4. Sensitivity of the Sensor Ferrogel to Ionic Strength

Figure 5 depicts the swelling levels of the sensor ferrogels over a wide range of varying ionic strengths from nM to 5 M.

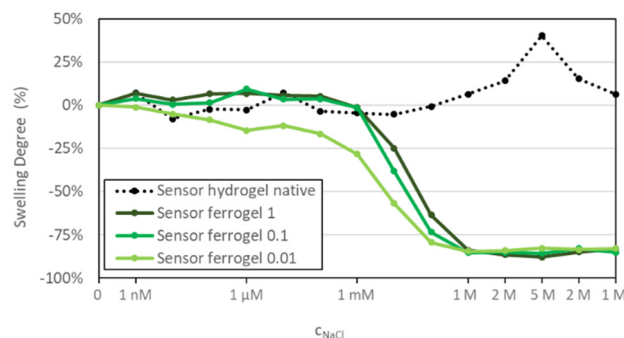


**Figure 5.** Swelling sensitivity of sensor ferrogels in NaCl solutions versus ionic strength.

A decay of the swelling curves between 1 mM and 1 M NaCl shows the concentration range of the deswelling that applies to all three dilution levels. Interesting for sensory applications is the flattened curve starting at 1 nM to 1 mM of the 1:100 sample. For this ferrogel, there seems to be an optimal balance between the charge density of ionized iron oxide particles under changing ionic strength and the mechanical stability of the hydrogel, so it can be used as a stimuli-responsive ferrogel in sensory applications.

#### 4. Conclusions

The use of different cross-linked hydrogels as templates for the wet chemical precipitation of iron oxide producing fairly homogeneous cubic-shaped particles with superparamagnetic characteristic curves independent of the applied concentration of iron salts and base was presented. The ion-sensitive swelling properties of the sensor ferrogels and the reversibility of their swelling make them suitable candidates for applications in piezoresistive sensors. Their magnetic properties allow applications under magnetic field control in microfluidics and medicine. Due to their strong swelling in water, the lower cross-linked actuator ferrogels could be used as adsorption materials for the remediation of contaminated water.

**Supplementary Materials:** The following are available online at <https://www.mdpi.com/article/10.3390/chemproc2021005049/s1>.

**Author Contributions:** Conceptualization, A.M., D.F. and M.G.; methodology, A.M., S.W. and M.S.; writing—original draft preparation, A.M.; writing—review and editing, D.F., M.S., S.O. and G.G.; supervision, D.F. and M.G.; project administration, G.G.; funding acquisition, G.G. All authors have read and agreed to the published version of the manuscript.

**Funding:** This research was funded by the German Research Foundation (DFG) in the course of the Research Training Group “Hydrogel-Based Microsystems” (RTG 1865).

**Institutional Review Board Statement:** Not applicable.

**Informed Consent Statement:** Not applicable.

**Data Availability Statement:** Not applicable.

**Acknowledgments:** We thank the Institute of Electronic Packaging Technology (German abbreviation IAVT) at TU Dresden for the access to their scanning electron microscope (SEM).

**Conflicts of Interest:** The authors declare no conflict of interest.

#### References

1. Guenther, M.; Gerlach, G. *Hydrogels for Chemical Sensors*; Springer: Berlin/Heidelberg, Germany, 2009. [CrossRef]
2. Hines, L.; Petersen, K.; Lum, G.Z.; Sitti, M. Soft Actuators for Small-Scale Robotics. In *Advanced Materials*; Wiley-VCH: Hoboken, NJ, USA, 2017; p. 1603483. [CrossRef]
3. Bobik, M.; Korus, I.; Dudek, L. The Effect of Magnetite Nanoparticles Synthesis Conditions on Their Ability to Separate Heavy Metal Ions. *Arch. Environ. Prot.* **2017**, *43*, 3–9. [CrossRef]
4. Darezereshki, E.; Khodadadi Darban, A.; Abdollahy, M.; Jamshidi-Zanjani, A. Influence of Heavy Metals on the Adsorption of Arsenate by Magnetite Nanoparticles: Kinetics and Thermodynamic. *Environ. Nanotechnol. Monit. Manag.* **2018**, *10*, 51–62. [CrossRef]
5. Hayashi, K.; Matsuyama, T.; Ida, J. A Simple Magnetite Nanoparticle Immobilized Thermoresponsive Polymer Synthesis for Heavy Metal Ion Recovery. *Powder Technol.* **2019**, *355*, 183–190. [CrossRef]
6. Sivudu, K.S.; Rhee, K.Y. Preparation and Characterization of PH-Responsive Hydrogel Magnetite Nanocomposite. *Colloids Surf. A Physicochem. Eng. Asp.* **2009**, *349*, 29–34. [CrossRef]
7. Zhao, W.; Odellius, K.; Edlund, U.; Zhao, C.; Albertsson, A.C. In Situ Synthesis of Magnetic Field-Responsive Hemicellulose Hydrogels for Drug Delivery. *Biomacromolecules* **2015**, *16*, 2522–2528. [CrossRef] [PubMed]
8. Liu, T.Y.; Hu, S.H.; Liu, K.H.; Liu, D.M.; Chen, S.Y. Preparation and Characterization of Smart Magnetic Hydrogels and Its Use for Drug Release. *J. Magn. Magn. Mater.* **2006**, *304*, 397–399. [CrossRef]
9. Kim, J.H.; Jang, J.W.; Jo, Y.H.; Abdi, F.F.; Lee, Y.H.; Van De Krol, R.; Lee, J.S. Hetero-Type Dual Photoanodes for Unbiased Solar Water Splitting with Extended Light Harvesting. *Nat. Commun.* **2016**, *7*, 13380. [CrossRef] [PubMed]
10. Tilley, S.D.; Cornuz, M.; Sivula, K.; Grätzel, M. Light-Induced Water Splitting with Hematite: Improved Nanostructure and Iridium Oxide Catalysis. *Angew. Chem. Int. Ed.* **2010**, *49*, 6405–6408. [CrossRef] [PubMed]
11. Liu, X.; Liu, J.; Lin, S.; Zhao, X. Hydrogel Machines. *Mater. Today* **2020**, *36*, 102–124. [CrossRef]
12. Krishnan, K.M. Biomedical Nanomagnetism: A Spin through Possibilities in Imaging, Diagnostics, and Therapy. *IEEE Trans. Magn.* **2010**, *46*, 2523–2558. [CrossRef]
13. Muya, F.N.; Sunday, C.E.; Baker, P.; Iwuoha, E. Environmental Remediation of Heavy Metal Ions from Aqueous Solution through Hydrogel Adsorption: A Critical Review. *Water Sci. Technol.* **2016**, *73*, 983–992. [CrossRef] [PubMed]
14. Erfkamp, J.; Guenther, M.; Gerlach, G. Hydrogel-Based Sensors for Ethanol Detection in Alcoholic Beverages. *Sensors* **2019**, *19*, 1199. [CrossRef] [PubMed]

15. Keplinger, C.; Sun, J.Y.; Foo, C.C.; Rothmund, P.; Whitesides, G.M.; Suo, Z. Stretchable, Transparent, Ionic Conductors. *Science* **2013**, *341*, 984–987. [[CrossRef](#)] [[PubMed](#)]
16. Unni, M.; Rinaldi, C. Chapter 4: Magnetic characterization of iron oxide nanoparticles for biomedical applications. In *Biomedical Nanotechnology*; Humana Press: New York, NY, USA, 2017. [[CrossRef](#)]
17. Teja, A.; Koh, P.Y. Synthesis, Properties, and Applications of Magnetic Iron Oxide Nanoparticles. *Prog. Cryst. Growth Charact. Mater.* **2009**, *55*, 22–45. [[CrossRef](#)]
18. Li, W.; Zhao, H.; Teasdale, P.R.; John, R.; Zhang, S. Synthesis and Characterisation of a Polyacrylamide-Polyacrylic Acid Copolymer Hydrogel for Environmental Analysis of Cu and Cd. *React. Funct. Polym.* **2002**, *52*, 31–41. [[CrossRef](#)]